Interference patterns of Bose-condensed gases in a two-dimensional optical lattice



2003 J. Phys. B: At. Mol. Opt. Phys. 36 2083

(http://iopscience.iop.org/0953-4075/36/10/316)

INSTITUTE OF PHYSICS PUBLISHING JOURNAL OF PHYSICS B: ATOMIC, MOLECULAR AND OPTICAL PHYSICS

J. Phys. B: At. Mol. Opt. Phys. **36** (2003) 2083–2092 PII: S0953-4075(03)57141-3

# Interference patterns of Bose-condensed gases in a two-dimensional optical lattice

**Shujuan Liu**[1], **Hongwei Xiong**[1], **Zhijun Xu**[1] **and Guoxiang Huang**[2]

[1] Department of Applied Physics, Zhejiang University of Technology, Hangzhou 310032, China
[2] Department of Physics and Key Laboratory for Optical and Magnetic Resonance Spectroscopy, East China Normal University, Shanghai 200062, China

Received 27 November 2002, in final form 14 March 2003
Published 7 May 2003
Online at stacks.iop.org/JPhysB/36/2083

**Abstract**

For a Bose-condensed gas confined in a magnetic trap and in a two-dimensional (2D) optical lattice, the non-uniform distribution of atoms in different lattice sites is considered based on the Gross–Pitaevskii equation. A propagator method is used to investigate the time evolution of 2D interference patterns after (i) only the optical lattice is switched off, and (ii) both the optical lattice and the magnetic trap are switched off. An analytical description on the motion of side peaks in the interference patterns is presented by using the density distribution in a momentum space.

## 1. Introduction

In the last few years, due to the experimental realization of Bose–Einstein condensation in 1995 [1], we have witnessed remarkable experimental and theoretical advances in the study of ultra-cold Bose gases [2]. Recently, a Bose-condensed gas confined in an optical lattice (created by retroreflected laser beams) and in a magnetic trap has been investigated (see [3] and references therein). In such a system, many subcondensates form and they are confined in the minima of the optical lattice potential. This provides an ideal system for investigating many interesting properties of the Bose–Einstein condensate (BEC), such as the quantum transition from a superfluid to a Mott insulating state of a ultra-cold Bose gas [4].

The coherence property of a BEC confined in an optical lattice and in a magnetic trap can be obtained by observing the time evolution of the interference patterns when both the optical lattice and the magnetic trap are switched off. The interference patterns obtained in this way are similar to the diffraction patterns of coherent light from a grating. For the BECs in one-dimensional (1D) [5], two-dimensional (2D) [6] and three-dimensional (3D) [4] optical lattices, the interference patterns are clearly shown experimentally. In [4], the quantum transition from a superfluid to a Mott insulating state is confirmed by observing the characters of the interference patterns.

In a recent experiment, Müller *et al* [7] studied the time evolution of the interference patterns when only a 1D optical lattice is switched off. It is shown that, due to the presence

  

of the magnetic trap, there is a periodic harmonic motion in the side peaks. This gives us a new opportunity to investigate the properties of the coherent matter wave such as the collision between the side peaks. In our previous work [8], a propagator method was used to study the time evolution of the interference patterns formed in a 1D optical lattice and the harmonic motion of the side peaks predicted is in agreement with the experimental result given in [7]. In the present work, we generalize the method developed in [8] to a 2D case, i.e. we consider the time evolution of the interference patterns for a Bose-condensed gas confined in a 2D optical lattice and in a magnetic trap, with the emphasis especially on the situation when only the optical lattice is switched off.

## 2. A Bose-condensed gas in combined trapping potentials

For the Bose-condensed gas confined in a 2D optical lattice and a magnetic trap with an axial symmetry along the $z$ axis, the dynamics of the condensate at low temperature is described by the well-known Gross–Pitaevskii equation [3]:

$$\mathrm{i}\hbar\frac{\partial\Psi}{\partial t} = \left[-\frac{\hbar^2}{2m}\nabla^2 + \frac{1}{2}m\omega_\perp^2(x^2+y^2) + \frac{1}{2}m\omega_z^2 z^2 + V_{latt} + g|\Psi|^2\right]\Psi, \tag{1}$$

where $\omega_\perp$ and $\omega_z$ are, respectively, the harmonic angular frequencies of the magnetic trap in the radial and axial directions and $g = 4\pi^2\hbar^2 a_s/m$ with $a_s$ the s-wave scattering length. When the polarization vectors of two perpendicular optical standing waves are orthogonal, the 2D optical lattice potential takes the form [6]

$$V_{latt} = U_0\left[\sin^2\left(\frac{2\pi x}{\lambda}\right) + \sin^2\left(\frac{2\pi y}{\lambda}\right)\right], \tag{2}$$

where $U_0$ denotes the depth of the optical lattice which can be increased by increasing the intensity of retroreflected laser beams, while $\lambda$ is the wavelength of the retroreflected laser beams. We consider here the case of $\omega_\perp \ll \omega_z$ and hence the condensate is disc-shaped with a larger extension in the $x$ and $y$ directions when in the presence of only the magnetic trap. After the optical lattice potential $V_{latt}$ is switched on a number of subcondensates appear which are confined in the minima (lattice sites) of the optical lattice potential. For the optical lattice created by the laser beams with wavelength $\lambda$, $d = \lambda/2$ is the period of the optical lattice potential, which can be regarded as the distance between two neighbouring lattice sites.

We assume that the width of subcondensates in each lattice site, $\sigma$, is much less than $d$, which can be realized in the present experiment by simply increasing the depth of the optical lattice. We consider here the case that the subcondensates in different lattice sites are fully coherent, i.e. the chemical potential of these subcondensates is identical and hence the condensed state wavefunction (or order parameter, as it will be called) $\Psi$ of the overall subcondensates can be written as

$$\Psi = \sum_{k_x,k_y}\Phi_{k_xk_y}(x,y,z)\mathrm{e}^{-\mathrm{i}\mu t/\hbar}, \tag{3}$$

where $\mu$ is the chemical potential and $k_j$ $(j = x, y)$ denotes the $k_j$th lattice site in the $j$th direction.

Substituting (3) into equation (1), we have

$$\left[-\frac{\hbar^2}{2m}\nabla^2 + \frac{1}{2}m\omega_\perp^2(x^2+y^2) + \frac{1}{2}m\omega_z^2 z^2 + V_{latt} + g|\Phi_{k_xk_y}|^2\right]\Phi_{k_xk_y} = \mu\Phi_{k_xk_y}. \tag{4}$$

In obtaining equation (4) we have used the condition that the overlap between neighbouring subcondensates can be neglected in the case of $\sigma \ll d$. To illustrate the character of

$\Phi_{k_xk_y}$ clearly, using the coordinate transformation $x - k_xd \to x$, $y - k_yd \to y$ and making a Taylor expansion of the optical lattice potential to the quadratic terms with respect to the lattice site $\{k_x, k_y\}$, it is straightforward to get the following equation:

$$\left[-\frac{\hbar^2}{2m}\nabla^2 + \frac{1}{2}m\omega_\perp^2((x+k_xd)^2+(y+k_yd)^2) + \frac{1}{2}m\omega_z^2z^2 + \tfrac{1}{2}m\tilde{\omega}_\perp^2(x^2+y^2) + g|\Phi_{k_xk_y}|^2\right]\Phi_{k_xk_y} = \mu\Phi_{k_xk_y}. \quad (5)$$

Equation (5) determines the wavefunction $\Phi_{k_xk_y}$ at the lattice site $(k_x, k_y)$. In the present experiment, the intensity of the retroreflected laser can be increased so that one can have $\tilde{\omega}_\perp \gg \omega_\perp$. For the subcondensate confined in the lattice sites, one has $-d/2 < x < d/2$ and $-d/2 < y < d/2$. Thus we obtain $x \ll k_xd$ and $y \ll k_yd$ except for the subcondensate in the central lattice site. As a result the term $\frac{1}{2}m\omega_\perp^2((x+k_xd)^2+(y+k_yd)^2)$ in equation (5) can be approximated as $\frac{1}{2}m\omega_\perp^2(k_x^2d^2+k_y^2d^2)$. As for the subcondensate in the central lattice site, because $\tilde{\omega}_\perp \gg \omega_\perp$, the above approximation is valid too. Thus equation (5) can be reduced to

$$\left[-\frac{\hbar^2}{2m}\nabla^2 + \frac{1}{2}m\omega_z^2z^2 + \frac{1}{2}m\tilde{\omega}_\perp^2(x^2+y^2) + g|\Phi_{k_xk_y}|^2\right]\Phi_{k_xk_y} = \mu_{k_xk_y}\Phi_{k_xk_y}, \quad (6)$$

where $\mu_{k_xk_y} = \mu - \frac{1}{2}m\omega_\perp^2d^2(k_x^2+k_y^2)$, which can be regarded as an effective chemical potential of the subcondensate on the lattice site $\{k_x, k_y\}$. Assuming that $\mu = \frac{1}{2}m\omega_\perp^2d^2k_M^2$, the effective chemical potential then is

$$\mu_{k_xk_y} = \tfrac{1}{2}m\omega_\perp^2d^2(k_M^2 - k_x^2 - k_y^2). \quad (7)$$

Because the occupied lattice sites lie within a circle, $\pi k_M^2$ can be regarded as the number of subcondensates induced by the optical lattice.

In the present work, we are interested in the case $\hbar\omega_z \ll \mu \ll \hbar\tilde{\omega}_\perp$. In this situation, each subcondensate in the optical lattice is a cigar-shaped one along the $z$ direction. Thus it displays a quasi-1D character. So a Thomas–Fermi approximation can be applied in the $z$ direction. After integrating out the fast-varying variables $x$ and $y$ in equation (6), one obtains [9]

$$\left[-\frac{\hbar^2}{2m}\frac{d^2}{dz^2} + \frac{1}{2}m\omega_z^2z^2 + g_{1D}|\varphi_{k_xk_y}(z)|^2\right]\varphi_{k_xk_y}(z) = \mu_{k_xk_y}\varphi_{k_xk_y}(z), \quad (8)$$

where $\varphi_{k_xk_y}(z)$ is the wavefunction of the subcondensate at the lattice site $(k_x, k_y)$ in the $z$ direction and $g_{1D} = 2\hbar^2a_s/m\tilde{l}_\perp^2$ ($\tilde{l}_\perp = (\hbar/m\tilde{\omega}_\perp)^{1/2}$) is an effective coupling constant in one dimension.

In the $z$ direction, using the Thomas–Fermi approximation we obtain the atomic number $N_{k_xk_y}$ in the lattice site $\{k_x, k_y\}$ as

$$N_{k_xk_y} = \frac{4\sqrt{2}\mu_{k_xk_y}^{3/2}}{3g_{1D}m^{1/2}\omega_z}. \quad (9)$$

Thus the ratio between the atomic number in the lattice site $(k_x, k_y)$ and the atomic number in the central lattice site $(0, 0)$ is

$$N_{k_xk_y} = N_{00}\left(1 - \frac{k_x^2+k_y^2}{k_M^2}\right)^{3/2}. \quad (10)$$

We see that the uniform chemical potential of the fully coherent subcondensates and the presence of the magnetic trap result in a non-uniform distribution of the atomic number in different lattice sites. It is worth pointing out that the atoms can move from one lattice site to

another when the subcondensates are fully coherent (i.e. the system is in a superfluid state). Thus the atomic number in lattice sites discussed here should be regarded as an average one. In addition, the value of $k_M$ can be obtained by considering the condition $N_0 = \sum'_{k_x,k_y} N_{k_x k_y}$. Here $N_0$ is the total atomic number in all subcondensates and the prime in the sum means that the summation about $k_x$, $k_y$ should satisfy the condition $k_x^2 + k_y^2 \leqslant k_M^2$. Based on this analysis, $k_M$ is given by

$$k_M = \left(\frac{15N_0 g_{1D}\omega_z}{4\pi m\omega_\perp^3 d^3}\right)^{1/5}. \tag{11}$$

In the present work, the parameters used are $\omega_\perp = 24 \times 2\pi$ Hz, $\omega_z = 220 \times 2\pi$ Hz and $\tilde{\omega}_\perp = 10^4 \times 2\pi$ Hz for $N_0 = 10^5$ $^{87}$Rb atoms. Note that $\tilde{\omega}_\perp$ here is about one-half of the experimental value used in [6]. Thus the subcondensates discussed here are fully coherent. It is obvious that the condition $\hbar\omega_z \ll \mu \ll \hbar\tilde{\omega}_\perp$ used above holds for these parameters.

## 3. The Bose-condensed gas in a momentum space

We now investigate the density distribution of the Bose-condensed gas in a momentum space. Note that, for the parameters used here, the Thomas–Fermi approximation is no longer valid in the $x$ and $y$ directions. For a larger value of $U_0$ it is reasonable to assume that the density distribution of subcondensates in the optical lattice has a form of Gaussian distribution in $x$–$y$ coordinate space, i.e. $\Phi_0(x, y) \sim \sum'_{k_x,k_y} \exp[-((x - k_x d)^2 - (y - k_y d)^2)/2\sigma^2]$. Due to the periodicity of the lattice, the wavefunction in momentum space takes the form

$$\Psi_0(p_x, p_y) = \Phi_0(p_x, p_y)\frac{\sin[(2k_M + 1)p_x d/\hbar]}{\sin p_x d/2\hbar}\frac{\sin[(2k_M + 1)p_y d/\hbar]}{\sin p_y d/2\hbar}, \tag{12}$$

where $\Phi_0(p_x, p_y) \sim \exp[-(p_x^2 + p_y^2)\sigma^2/2\hbar^2]$. We see that the momentum distribution of the Bose-condensed gas exhibits sharp peaks at $p_j = 2\pi n_j\hbar/d$ ($j = x, y$). The width of each peak in momentum space can be approximated as $\Delta p_j \sim \pi\hbar/(2k_M + 1)d$. From this character one can obtain directly the following results.

(i) As pointed out in [5, 8], the density distribution of the subcondensates in momentum space provides important information on the evolution of interference patterns. The presence of sharp peaks in the momentum distribution of the condensate with nonzero $n_j$ implies that there would be side peaks in coordinate space after the optical lattice is switched off. The classical approximation of the initial velocity $v_j = p_j/m$ can give a quite good description for the motion of the side peaks. When only the optical lattice is switched off, due to the presence of the magnetic trap the harmonic motion of the centre of mass of the side peaks is given by

$$\boldsymbol{r}_{n_x,n_y} = \frac{2\pi n_x\hbar}{m\omega_\perp d}\sin(\omega_\perp t)\boldsymbol{e}_x + \frac{2\pi n_y\hbar}{m\omega_\perp d}\sin(\omega_\perp t)\boldsymbol{e}_y, \tag{13}$$

where $\boldsymbol{e}_x$ and $\boldsymbol{e}_y$ are two unit vectors along the $x$ and $y$ directions. When both the optical lattices and magnetic trap are switched off, the motion of the side peaks is given by

$$\boldsymbol{r}_{n_x,n_y} = \frac{2\pi n_x\hbar t}{md}\boldsymbol{e}_x + \frac{2\pi n_y\hbar t}{md}\boldsymbol{e}_y. \tag{14}$$

(ii) From the density distribution in momentum space $n(p_x, p_y) = |\Phi_0(p_x, p_y)|^2$, the relative population of the side peaks with respect to the central peak can be approximated by $\exp[-4\pi^2(n_x^2 + n_y^2)\sigma^2/d^2]$. This formula is very useful when experimental parameters are chosen to observe clearly the side peaks in the interference patterns.

## 4. Density distribution of the condensate after switching off only the optical lattice

In [8], the evolution of interference patterns of the subcondensates induced by a 1D optical lattice is investigated when only the optical lattice is switched off. In this section, we generalize the method developed in [8] to consider the evolution of the interference pattern when switching off only the 2D optical lattice. Using the density distribution in coordinate space and the result given by equation (10), the normalized wavefunction of the Bose-condensed gas at time $t = 0$ takes the form

$$\Psi(x, y, z, t = 0) = A_n \sum_{k_x, k_y}{}' \Phi_{k_x k_y}(x, y, t = 0)\Phi_{k_x k_y}(z, t = 0) \tag{15}$$

and where $A_n = \sqrt{5/2}/\pi\sigma k_M$ is a normalization constant. In the above equation, $\Phi_{k_x k_y}(z, t = 0)$ represents the normalized wavefunction in the $z$ direction, and $\Phi_{k_x k_y}(x, y, t = 0)$ is given by

$$\Phi_{k_x k_y}(x, y, t = 0) = \left(1 - \frac{k_x^2 + k_y^2}{k_M^2}\right)^{3/4} \mathrm{e}^{-((x-k_x d)^2+(y-k_y d)^2)/2\sigma^2}. \tag{16}$$

Note that the factor $(1 - (k_x^2 + k_y^2)/k_M^2)^{3/4}$ in the above expression reflects the non-uniform distribution of atoms in the lattice which is given by equation (10).

When the optical lattice is switched off, the evolution of a interference pattern can be illustrated by considering the density distribution $n(x, y, t)$ in $x$–$y$ coordinate space:

$$n(x, y, t) = N_0 \int |\Psi(x, y, z, t)|^2 \,\mathrm{d}z = N_0 |\Psi(x, y, t)|^2. \tag{17}$$

In the case of the effective chemical potential $\mu_{k_x k_y}$ being much smaller than the ground state energy $\hbar\tilde{\omega}_\perp/2$ of the atoms in the lattice site $(k_x, k_y)$, the noninteracting model can provide a good description [5, 8]. When neglecting the interatomic interaction, the normalized wavefunction $\Psi(x, y, t) = A_n \sum'_{k_x, k_y} \Phi_{k_x k_y}(x, y, t)$ can be obtained through the well-known propagator method [8]. Recently, the vortex dynamics of parabolically confined Bose gases is also investigated by the propagator method [10]. Using this technique the condensed state wavefunction at time $t$ can be obtained by using the following integral equation [11]:

$$\Psi(x, y, t) = \int_{-\infty}^{\infty} K(x, y, t; x_1, y_1, t = 0)\Psi(x_1, y_1, t = 0)\,\mathrm{d}x_1\,\mathrm{d}y_1, \tag{18}$$

where the propagator $K(x, y, t; x_1, y_1, t = 0)$ is given by

$$K(x, y, t; x_1, y_1, t = 0) = \prod_{j=x,y} K_j(r_j, t; r_{j1}, t = 0). \tag{19}$$

In the above equation, $r_x \equiv x (r_y \equiv y)$, $r_{x1} \equiv x_1 (r_{y1} \equiv y_1)$ and

$$K_j(r_j, t; r_{j1}, t = 0) = \left[\frac{m\omega_\perp}{2\pi \mathrm{i}\hbar \sin\omega_\perp t}\right]^{1/2} \exp\left\{\frac{\mathrm{i}m\omega_\perp}{2\hbar \sin\omega_\perp t}[(r_j^2 + r_{j1}^2)\cos\omega_\perp t - 2r_j r_{j1}]\right\}. \tag{20}$$

By equations (16) and (18) it is straightforward to get the following analytical result of $\Psi(x, y, t)$:

$$\Psi(x, y, t) = A_n \sum_{k_x, k_y}{}' \left(1 - \frac{k_x^2 + k_y^2}{k_M^2}\right)^{3/4} \prod_{j=x,y} \Xi_j(r_j, t), \tag{21}$$

where

$$\Xi_j(r_j,t)=\sqrt{\frac{1}{\sin\omega_\perp t(\cot\omega_\perp t+\mathrm{i}\gamma)}}\exp\left[-\frac{(k_jd\cos\omega_\perp t-r_j)^2}{2\sigma^2\sin^2\omega_\perp t(\cot^2\omega_\perp t+\gamma^2)}\right]$$
$$\times\ \exp\left[-\frac{\mathrm{i}(k_jd\cos\omega_\perp t-r_j)^2\cot\omega_\perp t}{2\gamma\sigma^2\sin^2\omega_\perp t(\cot^2\omega_\perp t+\gamma^2)}\right]$$
$$\times\ \exp\left[\frac{\mathrm{i}(r_j^2\cos\omega_\perp t+k_j^2d^2\cos\omega_\perp t-2k_jr_jd)}{2\gamma\sigma^2\sin\omega_\perp t}\right], \tag{22}$$

where the dimensionless parameter $\gamma=\hbar/m\omega_\perp\sigma^2$.

From the result given by equation (21), we see that the period of $\Psi(x,y,t)$ is $T=2\pi/\omega_\perp$, while the period of the density distribution $n(x,y,t)$ is $\pi/\omega_\perp$. The density at $x=0$, $y=0$ reaches a maximum value at time $t_m=(2m-1)\pi/\omega_\perp$ with $m$ a positive integer. At time $t_m$, $|\Psi(x=0,y=0,t_m)|^2$ is given by

$$|\Psi(x=0,y=0,t_m)|^2=\alpha^2_{\perp\text{-}ideal}=\frac{A_n^2}{\gamma^2}\left(\frac{4\pi k_M^2}{9}\right)^2. \tag{23}$$

According to the fact that there are only a small number of atoms in each lattice site, we assume here that the atoms in a subcondensate are in the ground state of the corresponding lattice site. Thus we have $\sigma=\sqrt{\hbar/2m\tilde{\omega}_\perp}$ and it is easy to verify that the parameters used here satisfy $\sigma\ll d$. This shows that in the derivation of equation (4) the condition $\sigma\ll d$ holds. From the result given by equations (21) and (22), one can obtain the density distribution of the interference pattern. Displayed in figure 1(a) is the density distribution $n(x,y,t)$ (in units of $N_0A_n^2$) at $t=0.3\pi/\omega_\perp$. Note that in all the figures plotted in this paper the coordinates $x$ and $y$ are measured in units of $d$. The central and side peaks are clearly shown in the figure. Due to the presence of the magnetic trap, there is a harmonic motion of the side peaks. Displayed in figures 1(b)–(d) are the central and side peaks of the interference pattern at $t=0.5\pi/\omega_\perp$. From the result shown in figure 1(b), we see that the central peak is a very sharp one, analogous to the case of a 1D optical lattice [8]. Shown in figure 2 is the evolution of the interference pattern at different times. The evolution in the width of the central and side peaks and the motion of the side peaks is obvious. Due to the presence of the magnetic trap, there is no obvious evolution in the $z$ direction.

## 5. Density distribution of the condensate after switching off the combined potentials

We now turn to discuss the time evolution of the interference patterns when both the magnetic trap and the optical lattice are switched off. In this case the propagator can be obtained by setting $\omega_\perp\to 0$ in equation (19). Thus we get

$$K_b(x,y,t;x_1,y_1,t=0)=\prod_{j=x,y}K_{bj}(r_j,t;r_{j1},t=0), \tag{24}$$

where

$$K_{bj}(r_j,t;r_{j1},t=0)=\left[\frac{2\pi\mathrm{i}\hbar t}{m}\right]^{-1/2}\exp\left\{\frac{\mathrm{i}m(r_j-r_{j1})^2}{2\hbar t}\right\}. \tag{25}$$

The analytical result of $\Psi(x,y,t)$ is then

$$\Psi(x,y,t)=A_n{\sum_{k_x,k_y}}'\left(1-\frac{k_x^2+k_y^2}{k_M^2}\right)^{3/4}\prod_{j=x,y}\Xi_{bj}(r_j,t), \tag{26}$$

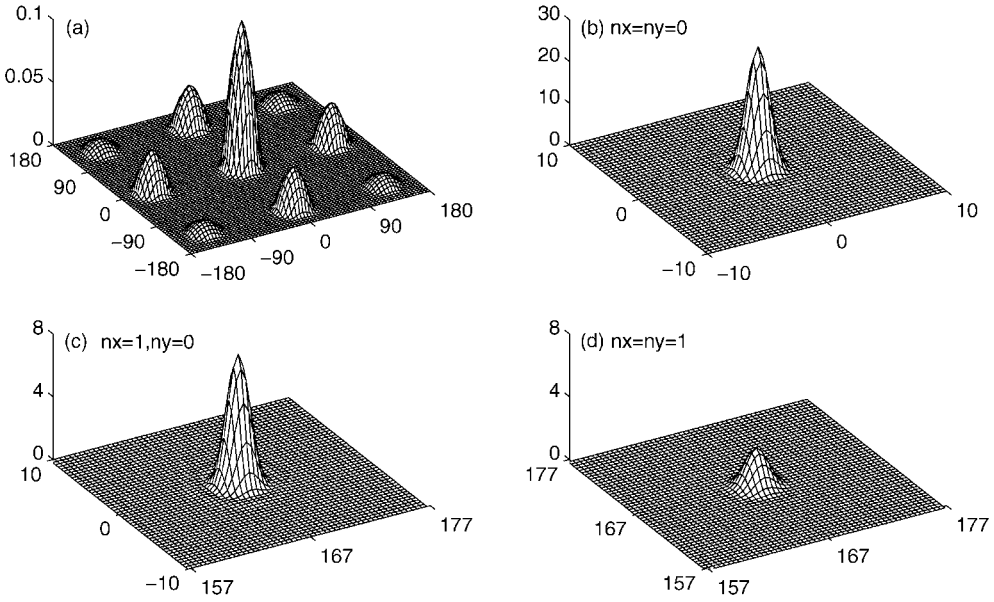


**Figure 1.** The interference patterns after only the 2D optical lattice is switched off. (a) shows the density distribution $n(x, y, t)$ (in units of $N_0 A_n^2$) at $t = 0.3\pi/\omega_\perp$. (b)–(d) show the central (b) and side peaks ((c) for $\{n_x = 1, n_y = 0\}$ and (d) for $\{n_x = 1, n_y = 1\}$) at $t = 0.5\pi/\omega_\perp$. In all the figures, the coordinates $x$ and $y$ are measured in units of $d$. Due to the presence of the magnetic trap, the central and side peaks are very sharp at $t = 0.5\pi/\omega_\perp$.

where

$$\Xi_{bj}(r_j, t) = \left(\frac{1}{1 + \mathrm{i}\Theta}\right)^{1/2} \exp\left[-\frac{(r_j - k_j d)^2}{2\sigma^2(1 + \Theta^2)}\right] \exp\left[\frac{\mathrm{i}(r_j - k_j d)^2}{2\sigma^2(\Theta + 1/\Theta)}\right], \quad (27)$$

where the dimensionless parameter $\Theta = \hbar t/m\sigma^2$. Shown in figure 3(a) is the density distribution (in units of $N_0 A_n^2$) at $t = 0.3\pi/\omega_\perp$. The density distribution at $t = 0.5\pi/\omega_\perp$ is given in figure 3(b). We see that the peaks are wider than those in the case when only the optical lattice is switched off. Displayed in figure 4 is the evolution of the interference pattern with the development of time.

As for the evolution in the $z$ direction, analogous to the case of the 1D optical lattice [5], one can find that the width $R_z(t)$ of the central peak is described by the asymptotic law $R_z(t) = R_z(0)\omega_z t$ after the central peak is formed.

## 6. Discussion and conclusion

The time evolution of the interference patterns of a Bose-condensed gas confined in a 2D optical lattice and a magnetic trap has been investigated by using a propagator method. Based on this method the analytical results of the condensed state wavefunction and motion of the side peaks have been provided. When the effective chemical potential in each lattice site is much smaller than $\hbar\tilde{\omega}_\perp$, a noninteracting model can give quite a good description of the evolution of the interference patterns. Nevertheless, the interaction between atoms can give an important correction to the central peak when only the optical lattice is switched off. After switching off the optical lattice, at time $t_m$ the central peak is very sharp and hence the interaction between atoms cannot be neglected. Generally speaking, starting directly from a general mean

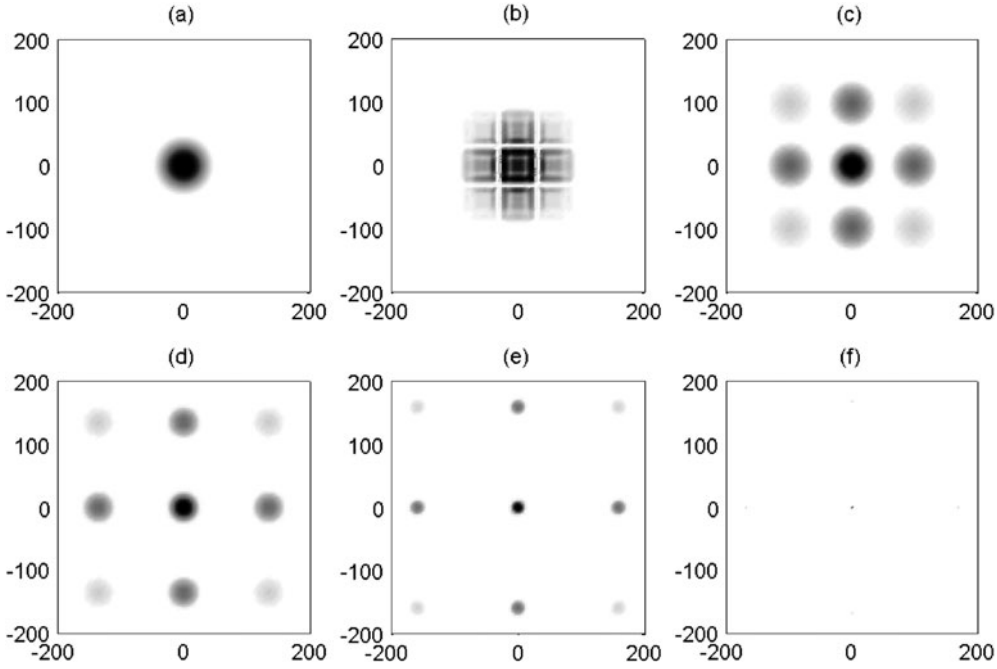


**Figure 2.** The evolution process of the central and side peaks after only the 2D optical lattice is switched off. The interference patterns are shown for different time-of-flight $t = 0$, $0.1\pi/\omega_\perp$, $0.2\pi/\omega_\perp$, $0.3\pi/\omega_\perp$, $0.4\pi/\omega_\perp$ and $0.5\pi/\omega_\perp$.

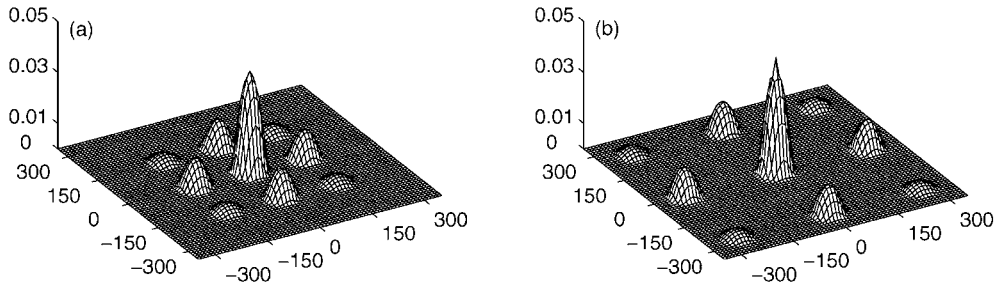


**Figure 3.** The interference patterns after both the 2D optical lattice and the magnetic trap are switched off. (a) and (b) show the interference patterns for $t = 0.3\pi/\omega_\perp$ and $0.5\pi/\omega_\perp$, respectively. The density distribution $n(x, y, t)$ is measured by $N_0 A_n^2$, while the coordinates $x$ and $y$ are in units of $d$.

field theory, one can give the interaction correction to the density distribution of the central peak. However, this would be a challenging process due to the fact that there is no single phase for the central peak due to the evolution of the wavepacket. In [8], for a 1D optical lattice a simple method is developed to investigate the interaction correction by using a Gaussian density distribution of the central peak and energy conservation. In the case of the 2D optical lattice, the analysis is similar and the interaction correction to the maximum density of the central peak at $t_m$ can be calculated straightforwardly. Assuming that $\beta$ denotes the ratio of the density at $x = 0$, $y = 0$ between the weakly interacting and noninteracting interference

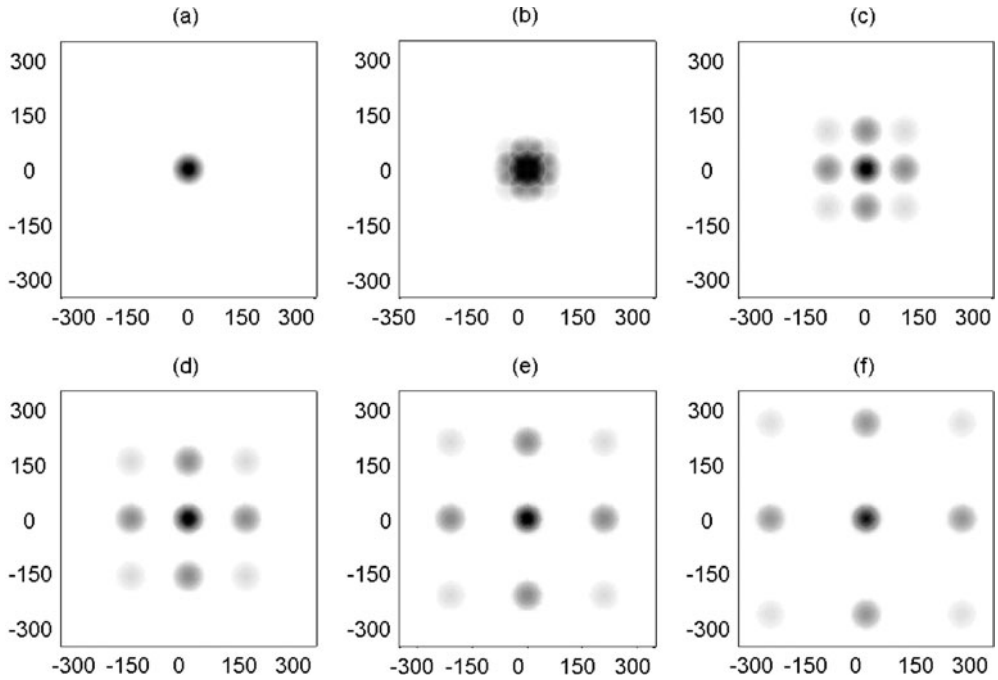


**Figure 4.** The evolution process of the central and side peaks for different time-of-flight $t = 0$, $0.1\pi/\omega_\perp$, $0.2\pi/\omega_\perp$, $0.3\pi/\omega_\perp$, $0.4\pi/\omega_\perp$ and $0.5\pi/\omega_\perp$ after both the 2D optical lattice and the magnetic trap are switched off.

patterns, at $t_m$ we have

$$\beta = \frac{1}{1 + E_{int}(\alpha_{\perp\text{-}ideal})/E_{all}}, \tag{28}$$

where $\alpha_{\perp\text{-}ideal}$ is given in equation (23), with

$$E_{all} = N_0\left(\frac{\hbar^2}{2m\sigma^2} + \frac{1}{2}m\tilde{\omega}_\perp^2\sigma^2\right), \tag{29}$$

and

$$E_{int}(\alpha_{\perp\text{-}ideal}) = \frac{9N_0^2 g\alpha_{\perp\text{-}ideal}^2\omega_z}{60k_M d\omega_\perp}. \tag{30}$$

For the parameters used here, a simple calculation shows that $\beta = 0.43$. We see that, quite differently from the case of 1D optical lattices (see [8]), the weak interaction between atoms results in a change in a deep way for the density of the central peak. This is not a surprising result due to the fact that, in the case of the 2D optical lattice, the central peak is cigar-shaped, while the central peak is disc-shaped for 1D optical lattices. Another possible interaction correction to the central peak at time $t_m$ would be a four-wave mixing which deserves detailed study in the future.

In addition, the interaction between atoms plays an important role in the colliding process of the side peaks, and this would be an interesting problem, deserving to be explored further. In the case of the Bose-condensed gas in a 1D optical lattice, the collisional haloes have been observed in the experiment [7]. When a 2D optical lattice is used to confine an axial symmetric Bose-condensed gas, there would be a collision between four side peaks, rather than

the collision between two side peaks, as in the case of a 1D optical lattice. This gives us a new opportunity to investigate the collision between side peaks both theoretically and experimentally. The method developed here can also be used straightforwardly to study the cigar-shaped Bose-condensed gas in a 2D optical lattice. For the cigar-shaped Bose-condensed gas, the harmonic angular frequencies of the magnetic trap is $\omega_x = \omega_z \gg \omega_y$. When the 2D optical lattice is imposed in the $x$ and $y$ directions, after the optical lattice is switched off the motion of the side peaks is given by

$$\boldsymbol{r}_{n_x,n_y} = \frac{2\pi n_x \hbar}{m\omega_\perp d}\sin(\omega_x t)\boldsymbol{e}_x + \frac{2\pi n_y \hbar}{m\omega_\perp d}\sin(\omega_y t)\boldsymbol{e}_y. \tag{31}$$

We see that the motion of the side peaks in $x$ and $y$ directions is quite different because $\omega_x \gg \omega_y$. In this case, the side peaks in the $x$ direction has a collision before that in the $y$ direction, and this gives us an opportunity for observing the collisions one after another. It is obvious that the method developed here can also be used to investigate the interference patterns of the Bose-condensed gases in a 3D optical lattice, which has been considered recently in [12] by using a different method.

## Acknowledgment

This work was supported by the Natural Science Foundation of China under grant nos 10205011 and 10274021.

## References

[1] Anderson M H *et al* 1995 *Science* **269** 198
Davis K B *et al* 1995 *Phys. Rev. Lett.* **75** 3969
Bradley C C *et al* 1995 *Phys. Rev. Lett.* **75** 1687
[2] Dalfovo F, Giorgini S, Pitaevskii L P and Stringari S 1999 *Rev. Mod. Phys.* **71** 463
[3] Morsch O and Arimondo E 2002 *Preprint* cond-mat/0209034
Burger S *et al* 2001 *Preprint* cond-mat/0111235
[4] Greiner M *et al* 2002 *Nature* **415** 39
Greiner M *et al* 2002 *Nature* **419** 51
[5] Pedri P *et al* 2001 *Phys. Rev. Lett.* **87** 220401
[6] Greiner M *et al* 2001 *Phys. Rev. Lett.* **87** 160405
[7] Müller J H *et al* 2002 *Preprint* cond-mat/0211079
[8] Xiong H *et al* 2002 *J. Phys. B: At. Mol. Opt. Phys.* **35** 4863
[9] Petrov D S, Shlyapnikov G V and Walraven J T M 2000 *Phys. Rev. Lett.* **85** 3745
Olshanii M 1998 *Phys. Rev. Lett.* **81** 938
[10] Tempere J and Devreese J T 2000 *Solid State Commun.* **113** 471
[11] Feynman R P and Hibbs A R 1965 *Quantum Mechanics and Path Integrals* (New York: McGraw-Hill)
[12] Adhikari S K and Muruganandam P 2002 *Preprint* cond-mat/0209429